HHS Public Access

Author manuscript

Cancer Lett. Author manuscript; available in PMC 2022 February 01.

Published in final edited form as:

Cancer Lett. 2019 April 10; 447: 24–32. doi:10.1016/j.canlet.2019.01.023.

RLIP inhibition suppresses breast-to-lung metastasis

Jyotsana Singhal[a,b], **Shireen Chikara**[a], **David Horne**[b], **Ravi Salgia**[a], **Sanjay Awasthi**[c], **Sharad S Singhal**[a,*]

[a]Department of Medical Oncology, City of Hope Comprehensive Cancer Center and National Medical Center, Duarte, CA 91010;

[b]Department of Molecular Medicine, City of Hope Comprehensive Cancer Center and National Medical Center, Duarte, CA 91010;

[c]Department of Internal Medicine, Texas Tech University Health Sciences Center, Lubbock, TX 79430

Abstract

Breast tumor metastasis is a leading cause of cancer-related deaths worldwide. Breast cancer (BC) cells frequently metastasize to the lungs, where they pose a formidable therapeutic challenge. In the current study, we evaluated the anti-proliferative and anti-metastatic effects of 2'-hydroxyflavanone (2HF) and RLIP inhibition in an array of triple-negative BC cell lines and an orthotopic mouse model of breast-to-lung metastasis. Compared to control treatment, RLIP inhibition reduced *in-vitro* cell viability and suppressed the migratory and invasive potential of BC cells. *In-vitro* studies showed that 2HF treatment reduced the expression of RLIP, KRAS, pERK, pSTAT3, and pP70S6K. Further, mice orthotopically implanted with lung-seeking luciferase-expressing TMD231 cells were treated with 2HF (50 mg/kg, b.w.), RLIP antisense (RAS; 5 mg/kg, b.w.), RLIP antibody (Rab; 5 mg/kg, b.w.) or a combination of 2HF+RAS+Rab. 2HF-, RAS-, and Rab-treated mice exhibited significantly lower primary tumor weight and reduced lung metastasis compared to control mice. Mice treated with a combination of 2HF+RAS+Rab exhibited no metastasis and significantly lower tumor weight than the single agent-treated mice. Collectively, our results suggest that 2HF has potential to be combined with RLIP inhibition/depletion to more effectively suppress primary breast tumor growth and metastasis to the lungs.

One Sentence Summary:

Our results suggest for the first time that RLIP inhibition/depletion suppresses primary breast tumor growth and metastasis to the lungs.

[*]**Address correspondence to:** Sharad S Singhal, Ph.D., Professor, Department of Medical Oncology, Beckman Research Institute of City of Hope, Duarte, CA 91010; Phone: 626-218-4238; ssinghal@coh.org.

Conflicts of interest: No conflict of interest exists for any of the authors.

Keywords

RLIP; breast cancer; phytochemicals; metastasis; lung; chemotherapeutics

1. Introduction

Breast cancer (BC) is one of the most common malignancies diagnosed in women, and metastatic BC maintains a high mortality rate despite improvement in clinical outcomes for patients with targeted primary tumors [1]. The 5-year survival rate for patients diagnosed with metastatic BC is a dismal 22% [1,2]. Even though the metastatic potential of triple-negative BC (TNBC) tumors, which do not express estrogen receptor (ER), progesterone receptor (PR), or HER-2, is similar to that of other BC types, TNBC is associated with poorer survival after recurrence [3]. This is primarily due to the aggressive nature of the disease and lack of hormone receptors that can serve as a therapeutic target. Therefore, the standard approach for TNBC treatment is the use of a taxanes, such as paclitaxel, which inflict considerable toxicity on healthy tissues [4]. Hence, there is a need to develop less toxic adjuvant therapies that can effectively target TNBC.

Several epidemiological studies have reported an inverse correlation between intake of citrus fruits and occurrence of BC [5–7]. Citrus fruits contain a complex mixture of phytochemicals with 2'-hydroxyflavanone (2HF) being the most abundant flavonoid. 2HF has demonstrated anticancer potential in *in-vitro* and *in-vivo* models of breast [8,9], bladder [10], colon [11], kidney [12,13], lung [14], and prostate [15,16] cancers. In our previous study, we demonstrated that 2HF exerts anticancer effects in BC cell lines (MCF7, MDA-MB231, and T47D) and reduces tumor growth in MDA-MB231 xenograft mouse models of BC [8]. Inhibition of tumor growth was accompanied by: (i) decreased phosphorylation (activation) of Akt, (ii) reduced expression of cell cycle-related proteins such as cyclin B1 and CDK4, (iii) decreased expression of anti-apoptotic proteins Bcl2 and survivin, (iv) increased expression of pro-apoptotic proteins Bax and cleaved PARP, (v) increased expression of E-cadherin, (vi) decreased levels of the angiogenesis marker CD31, and (vii) decreased expression of RAL-interacting protein (RLIP) [8]. However, the anti-metastatic potential of 2HF has not been studied in the context of breast cancer.

RLIP (encoded by *RALBP1;* [18p11.22]) has emerged as a promising target for cancer treatment, because it is overexpressed in a variety of cancer cell lines and tumor tissues [17,18]. RLIP is an ATP-dependent non-ATP-binding cassette (ABC) transporter that is responsible for the major transport function in many cells, including cancer cell lines, causing the efflux of glutathione (GSH)-electrophile conjugates (GS-Es) of both endogenous metabolites and environmental chemical toxins [17–24]. RLIP is essential for tumor growth and metastasis of melanomas [19], non-small cell lung cancer [20,21], renal cell carcinoma [24,25], and colon carcinomas [21]. Depletion of RLIP via small interfering RNA (siRNA)-mediated knockdown was associated with reduced tumor growth and metastasis in a xenograft mouse model of prostate cancer [26,27]. Similarly, lentiviral-based knockdown of RLIP decreased metastasis of UMUC3 cell to lungs in a xenograft mouse model of

bladder cancer [28]. These studies demonstrate the essential role of RLIP in tumorigenesis and cancer cell motility.

Therefore, the aim of the study was to investigate the anti-migratory potential of 2HF against TNBC cell lines *in-vitro* and *in-vivo*. We hypothesized that 2HF inhibits breast-to-lung metastasis by targeting RLIP, a protein that plays an important role in cancer cell motility. We studied the anti-migratory and anti-invasive effects of 2HF *in-vitro* in a panel of TNBC cell lines (MDA-MB231, MDA-MB231Br, and TMD231). We also investigated the anti-metastatic effects of 2HF, as well as targeted depletion/inhibition of RLIP via antisense and antibodies, *in-vivo* in a mouse model of BC after the orthotopic implantation of TMD231 (lung-seeking) cells genetically labeled with luciferase (luc). Our findings suggest that 2HF inhibits BC cell motility by targeting RLIP and its associated downstream signaling pathways.

2. Materials and methods

2.1. Reagents

2HF (purity ~99%), MTT, Horseradish peroxidase (HRP)-conjugated anti-mouse and anti-rabbit secondary antibodies were purchased from Sigma-Aldrich (St. Louis, MO). Antibodies against KRAS, pERK ($T^{202/204}$), pSTAT3 (Y^{705}), CD31, Ki67, cyclin B1, CDK4, Bcl2, survivin, Bim, Bax, vimentin, fibronectin, and E-cadherin were purchased from Santa Cruz Biotechnology (Columbus, OH) and Cell Signaling Technologies (Danvers, MA). CellTiter-Glo was procured from Promega (Madison, WI). The avidin/biotin complex detection kit was procured from Vector (Burlingame, CA). The universal *Mycoplasma* detection kit was purchased from American Type Culture Collection (ATCC; Manassas, VA). The RLIP antibodies and antisense were obtained as previously described [19,23]. D-luciferin was purchased from Goldbio (St. Louis, MO). AlamarBlue® was purchased from Thermo Fisher Scientific (Hanover Park, IL). The cell invasion assay kit was purchased from Cell Biolabs, Inc. (San Diego, CA).

2.2. Cell lines and culture

Human BC MDA-MB231 cell lines were purchased from ATCC. MDA-MB231Br (brain-seeking) and TMD231 (lung-seeking) BC cells were a kind gift from Dr. Harikrishna Nakshatri, Indiana University, IN. MDA-MB231, MDA-MB231Br, and TMD231 cells were cultured in Dulbecco's Modified Eagle's medium (DMEM) supplemented with 10% fetal bovine serum (FBS) and 1% penicillin/streptomycin (P/S) solution. The cell lines were authenticated by the Integrative Genomic Core of the Beckman Research Institute of City of Hope, Duarte, CA, by analyzing fifteen different human short tandem repeat (STRs), to test for interspecies contamination. Cells were also tested for *Mycoplasma* once every 3 months.

2.3. Luciferase transfection

The pLVX-EF1a-Luc-PgKpuro vector was used to produce the EF1a promoter-driven lentiviral luciferase vector. The virus was transduced into three BC cell lines (MDA-MB231, MDA-MB231Br, and TMD231). The transduced cells were screened with puromycin for

seven days. Three clones of each cell line were selected and tested for luciferase activity using the Promega Firefly luciferase kit (Promega Cat#E1500).

2.4. AlamarBlue® cell viability assay

Luc-transfected MDA-MB231-luc, MDA-MB231Br-luc, and TMD231-luc cells (5×10^3) were seeded into individual wells of a 96-well plate. Twenty-four h later, alamarBlue® was added to a final concentration of 10% and the plate was incubated at 37 °C for 4 h to get a baseline (Day 0) reading. Absorbance was measured at 570 and 600 nm. The cells were then washed with PBS, fresh medium supplemented with 10% FBS was added, and cells were treated with 2HF (ranging 0–100 μM). Every 24 h, alamarBlue® was added to a final concentration of 10%, and absorbency readings were taken after 4 h. Cell viability was determined by calculating the percent reduction in alamarBlue® over time for each treatment, as previously described [29]. The data shown represent mean cell viability under each treatment relative to control ± standard deviation for eight replicates per treatment for three independent experiments.

2.5. Cell migration assay

The ability of 2HF to inhibit the migration of MDA-MB231-luc and TMD231-luc cells was investigated using a wound healing assay. Cells were seeded into 6-well plates and grown to ~90% confluency. A sterilized 10-μl pipette tip was used to generate a wound across the cell monolayer. Cellular debris was washed with PBS, serum-free RPMI-1640 medium was added to each well, and the cells were treated with either vehicle or 2HF (50 μM). The open gap was photographed microscopically immediately and after 24 and 48 h. The migration ability of the cells was determined by measuring the width of the monolayer wound at three fields at 0, 24, and 48 h after scraping. The data shown represent the mean ± standard deviation of three independent experiments.

2.6. Cell invasion assay

The anti-migratory effects of 2HF on BC cells were studied *in-vitro* using a transwell Boyden chamber containing inserts with a polycarbonate membrane (8 μm pore size). Briefly, MDA-MB231-luc and TMD231-luc cells (0.5×10^6 cells/well), suspended in serum-free medium, were added to the upper chamber of the 24-well transwell plates and treated with either vehicle or 2HF (50 μM) for 24 h. DMEM supplemented with 10% FBS was added to the lower chamber. The plates were incubated in a humidified atmosphere with 95% air and 5% CO_2 at 37 °C. After indicated the time points, the non-migratory cells present on the inside of the insert were removed by wiping with a cotton swab dipped in PBS, and migratory cells attached to the underside of the insert were fixed with 4% paraformaldehyde for 15 min, permeabilized with 0.2% Triton X-100 in PBS, and stained with 0.2% crystal violet for 10 min at room temperature. The migratory cells in five random fields of the insert were photographed under a light microscope (200x). Later, the stained inserts were washed gently with water, transferred insert to an empty well, and cells were extracted using 200 μl of extraction buffer and then incubating 10 min on an orbital shaker. The number of invaded cells per membrane was determined by taking absorbance readings at 560 nm using a plate reader. The absorbance value was used to quantify the percentage of invasive 2HF-treated cells relative to vehicle-treated cells.

2.7. Western blot analysis of BC cells

MDA-MB231-luc, MDA-MB231Br-luc, and TMD231-luc BC cells (3×10^5 cells/well) were seeded in a 6-well plate. After a 24 h incubation, the cells were treated with either vehicle (DMSO) or 2HF (50 μM) for 24 h. The cells were harvested by trypsinization, centrifuged at 300 × *g* for 10 min. The resulting cell pellet was then lysed by brief sonication in 100 μl of SDS lysis buffer (Cell Signaling Technologies) containing protease and phosphatase inhibitors (Roche; Indianapolis, IN) to dissociate cell membranes. The protein samples were processed for Western blot analysis, as we described previously [8]. Change in the expression of the desired proteins (RLIP, pERK, KRAS, pP70S6K^{Thr389}, and pSTAT3^{Tyr705}) was determined by densitometric scanning of the immuno-reactive bands. Equal loading of proteins was confirmed by stripping and re-probing the membranes with β-actin antibodies. Western blot analysis was performed in triplicate and the image shown represents one typical replicate.

2.8. Orthotopic breast-to-lung metastasis mouse model

Female NOD scid gamma (NSG) mice (10 weeks old) obtained from the City of Hope Animal Resources Core Facility were housed in sterile conditions and allowed to acclimate to the laboratory conditions for one week prior to start of the experiment. The use and treatment of NSG mice was approved by the Institutional Animal Care and Use Committee (IACUC) at City of Hope National Medical Center, and the experiments were conducted in strict compliance with institutional regulations. A total of 56 female NSG homozygous mice were divided into 7 treatment groups (8 mice/ group) as follows: **(i)** corn oil, **(ii)** control antisense (CAS), **(iii)** pre-immune serum (PIS), **(iv)** 2HF, **(v)** RLIP antisense (RAS), **(vi)** RLIP antibody (Rab), and **(vii)** 2HF+RAS+Rab. Mice were anesthetized, and TMD231-luc cells (1×10^6 cells/0.1 ml) re-suspended in serum-free medium were injected into the fourth right mammary fatpad of each mouse. The animals were then subjected to bioluminescence imaging after intra-peritoneal (*i.p.*) injection of 3 mg D-luciferin in 0.1 ml of saline to verify successful tumor cell inoculation (Day 1). Treatment began on Day 2. The mice were treated with 2HF (50 mg/kg b.w.) in corn oil by oral gavage on alternate days; RLIP antisense and antibody (5 mg/kg b.w.) by *i.p.* weekly. Primary tumor's cross-sectional area was measured using calipers and body weights were recorded twice a week. Due to the large tumor size in mice in the control (corn oil, CAS, and PIS) groups, primary tumors from all mice were resected 33 days after cell implantation to decrease tumor burden and allow time for metastasis. *In-vivo bi*oluminescent imaging was conducted twice a week to monitor metastasis. After 51 days of treatment, mice were euthanized by CO_2 inhalation followed by cervical dislocation. The primary tumors were harvested and measured for tumor size and weight. The number of surface metastatic foci in the lungs and liver were counted and percent metastasis incidence was determined. Tumors from half of the mice for each group were paraformaldehyde-fixed and paraffin-embedded for immunohistochemistry. Tumors from the remaining mice were snap-frozen in liquid nitrogen and stored at −80°C for molecular analyses.

2.9. Western blot analysis of tumor tissue

Tumor tissues from control (corn oil, CAS, and PIS) and treatment (2HF, RAS, Rab, and 2HF+RAS+Rab) group mice were processed for Western blot analysis as we described previously [8]. Supernatant proteins were resolved by SDS-PAGE and transferred onto nitrocellulose membranes. The expression of the desired proteins was determined by densitometric scanning of the immuno-reactive bands. Equal loading of proteins was confirmed by stripping and re-probing the membranes with β-actin antibodies.

2.10. Histopathological examination of tumors for differentiation, proliferative, and angiogenic markers

Tumor tissues from control groups (corn oil, CAS, and PIS) and experimental groups (2HF, RAS, Rab, and 2HF+RAS+Rab) were fixed in buffered formalin for 12 h. Paraffin-embedded 5-μm thick tumor sections were prepared. Hematoxylin and eosin (H&E) staining to assess hyperplasia was performed on the paraffin-embedded tumor sections. Histopathologic analysis of proteins, such as E-cadherin and vimentin involved in epithelial-mesenchymal transition (EMT), CD31 to visualize blood vessels, Ki67 and RLIP to assess cell proliferation, and vimentin to analyze mesenchymal cells was performed using a Universal ABC detection kit (Vector). Immuno-reactivity is evidenced by a dark brown stain, whereas non-reactive areas display only the background color. Photomicrographs at 40x magnification were acquired using an Olympus DP72 microscope. Percent staining was determined by measuring positive immuno-reactivity per unit area. The intensity of antigen staining was quantified by digital image analysis using DP2-BSW software. Bars represent mean ± S.E. (n = 5); * $p<0.001$ compared with control.

2.11. Statistical Analysis

The data was analyzed using two-tailed unpaired Student's *t* tests and results are expressed as the mean ± SD. Changes in tumor size and body weight during the course of the experiments were visualized by scatter plot. The statistical significance of differences between control and treatment groups was determined by ANOVA followed by multiple comparison tests. Differences were considered statistically significant when the *p* value was < 0.05.

2.12. Ethics statement

No human subjects were involved in the present study. All animal studies were conducted upon approval by the City of Hope Animal Care and Ethics Committee, according to an IACUC-approved protocol. Any mice showing signs of distress, pain, or suffering due to tumor burden were humanely euthanized.

3. Results

3.1. 2HF treatment inhibits growth of BC cells

The growth inhibitory effects of 2HF on three BC cell lines (MDA-MB231-luc, MDA-MB231Br-luc, and TMD231-luc) were investigated using the alamarBlue® assay. The cell lines were treated with either the vehicle control (DMSO, <0.5%) or increasing

concentrations of 2HF (0–100 μM) for 0–4 days, and cell growth was assessed each day. 2HF induced a concentration and time-dependent decrease in the viability of all three cell lines, with IC_{50} values close to 50 μM at 72 h (Fig. 1)

3.2. 2HF exerts anti-migratory and anti-invasive effects on BC cells in-vitro

To test whether 2HF inhibits migration, a scratch wound healing assay was performed. MDA-MB231-luc and TMD231-luc cells were treated with either the vehicle control or 2HF (50 μM). Control MDA-MB231-luc and TMD231-luc cells demonstrated migration potential with 56% and 36% wound repair after 24 h, and 89% and 98% wound repair after 48 h, respectively (Fig. 2A). On the other hand, 2HF treatment (50 μM) of MDA-MB231-luc cells suppressed wound healing; with 48% and 64% wound closure after 24 and 48 h, respectively (Fig. 2A). For TMD231-luc cells, 2HF treatment resulted in 36% and 53% wound closure after 24 and 48 h, respectively (Fig. 2A).

In addition, the effect of 2HF treatment (50 μM) on cancer cell invasion after 24 h was studied using Matrigel® invasion chambers. As shown in Fig. 2B, the number of invading cells, as represented by crystal violet staining, was significantly lower among 2HF-treated MDA-MB231-luc and TMD231-luc cells as compared to vehicle-treated controls. These results suggest that 2HF inhibits the invasive potential of BC cells *in-vitro*.

3.3. 2HF affects protein expression levels in BC cells

In order to gain mechanistic insights into the molecular changes underlying the anti-growth, anti-migratory, and anti-invasive potential of 2HF, Western blot analysis was performed using MDA-MB231-luc, MDA-MB231Br-luc, and TMD231-luc cells were treated with vehicle or 2HF (50 μM) for 24 h, and protein expression changes for RLIP, pERK ($T^{202/204}$), KRAS, pP70S6K (T^{389}), pSTAT3 (Y^{705}) were studied. As expected, 2HF treatment caused a reduction in the expression of all proteins assessed in all three cell lines (Fig. 2C). This suggests that the anticancer mechanism of 2HF may involve the down-regulation of RLIP and KRAS and their associated signal transduction pathways, such as ERK, STAT3, and P70S6K, a downstream kinase in mTOR signaling.

3.4. 2HF suppresses tumor growth and breast-to-lung metastasis in an orthotopic mouse model in-vivo

The brain and lungs are the major sites for metastasis from primary breast tumors in most BC patients. Therefore, we next investigated if 2HF could suppress the migration of BC cells to lungs in an orthotopic mouse model. Upon implantation of TMD231-luc cells, bioluminescent imaging conducted on the same day (Day 1) confirmed the presence of localized cancer cells in animals (Fig. 3A). Starting the next day, the mice were treated with 2HF (50 mg/kg b.w.) via oral gavage on alternate days, or RLIP antisense (RAS) and RLIP antibody (Rab) (5 mg/kg b.w.) via *i.p.* administration weekly. In addition, we also evaluated the efficacy of combining 2HF with RAS and Rab (2HF+RAS+Rab) in suppressing breast tumor growth and metastasis. By Day 15 of treatment, slight differences in tumor growth were visible between mice in the control (corn oil, CAS, and PIS) and treatment (2HF, RAS, Rab, and 2HF+RAS+Rab) groups (Fig. 3A). By Day 29, administration of 2HF, RAS, Rab, and 2HF+RAS+Rab resulted in significantly lower tumor weight and size, as compared to

the control-treatment. Because primary tumors continue to grow rapidly before metastases are detectable, we resected primary tumors from all control and treatment groups' mice at 33 days post-implantation, before they became too large. Treatment with 2HF, RAS, and Rab alone caused a 58%, 60%, and 55% reduction in tumor size, respectively. Similarly, the 2HF+RAS+Rab combination treatment led to 69% decrease in tumor size (Fig. 3A). Treatment continued, following the same dose schedule after surgery.

Tumors began to recur in control and treatment group mice after excision of the primary tumors. As seen in Fig. 3A, mice in the control group exhibited primary tumor recurrence along with extensive metastasis in the lungs and liver at Day 51. Strikingly, primary tumors were remarkably smaller for mice in the treatment groups. Treatment with 2HF, RAS, and Rab alone resulted in tumors that were smaller than control tumors by 68%, 70%, and 67%, respectively. The combination treatment (2HF+RAS+Rab) resulted in tumors that were 78% smaller than control tumors at Day 51 (Fig. 3A). The mice in the control groups also had significantly more lung and liver metastasis than mice in the treatment groups. The incidence of lung metastasis was significantly lower in the 2HF, RAS, and Rab groups, and no visible lung or liver metastases were observed in the 2HF+RAS+Rab group (Figs. 3B and 3C). These data indicate that 2HF effectively slows primary breast tumor growth and suppresses tumor recurrence and metastasis by targeting RLIP. The suppression of metastasis by Rab- and RAS-induced RLIP inhibition/depletion confirms this conclusion.

3.5. Protein levels in tumor tissue following 2HF, RAS, Rab, and combination treatment

Tumor tissue lysates from mice in the control and treatment groups were assessed for proliferative, apoptotic, and cell cycle markers using Western blot and immunohistochemical analyses. Western blot analyses showed that 2HF treatment decreased protein expression levels of RLIP, inhibited phosphorylation (activation) of Akt and ERK, increased expression of Bax and E-cadherin, and decreased expression of Bcl2, vimentin, and CDK4 (Fig. 4). The H&E staining of primary tumor tissues from the control and treatment groups showed that 2HF, RAS, Rab and 2HF+RAS+Rab-treated mice exhibited less tumor growth compared to control mice (Fig. 5). In addition, H&E staining of other tissues, such as brain, heart, and kidney, showed no signs of toxicity in either the control or treatment group. Furthermore, H&E staining showed fewer metastatic foci in the lungs and liver of treated mice compared to control mice (Fig. 5). The immunohistochemical analysis of 2HF, RAS, Rab, and 2HF+RAS+Rab treated breast tumor sections, compared to control sections, showed lower levels of RLIP, the proliferation marker Ki67, the angiogenesis marker CD31, and the mesenchymal marker vimentin, with correspondingly higher levels of the epithelial differentiation marker E-cadherin (Fig. 6). Taken together, our results indicate that 2HF displays strong anticancer effects against BC tumors *in-vivo*.

4. Discussion

The objective of the present study was to evaluate the efficacy of 2HF in inhibiting breast-to-lung metastasis in a mouse model of triple-negative BC (TNBC). TNBC is highly refractory to therapy, and effective agents in clinical trials for metastatic TNBC including platinum agents, inflict toxicity to healthy tissues [3]. Therefore, treatment regimens that are non-

toxic to healthy tissues are needed. 2HF is a natural phytochemical with chemotherapeutic properties found in consumable citrus fruits [7]. In the present study, we have shown that in an orthotopic breast-to-lung mouse model, treatment with 2HF significantly inhibits primary tumor growth and metastasis to the lungs by targeting RLIP, a stress-responsive ATPase of the mercapturic acid pathway [22,23,30].

Previous studies found that 2HF inhibits the growth of SW620 and HCT116 human colon cancer cells and MCF7 BC cells via the induction of caspase-mediated apoptosis [11]. In A549 human lung cancer cell lines, 2HF inhibits the proliferation by arresting them in the G2/M phase of the cell cycle and simultaneously suppresses *in-vivo* lung cancer metastasis in immune deficient nude mice (BALB/c nu/nu mice) [14,31]. The anticancer effects of 2HF have also been linked to its ability to inactivate ERK and Akt/STAT3signaling pathways, repress androgen-responsiveness, and suppress angiogenesis by reducing vascular endothelial growth factor (VEGF) expression [6–16,31]. Consistent with above findings, we previously showed that 2HF inhibits BC growth and results in G2/M phase cell cycle arrest, followed by the induction of apoptosis [8]. This suggests that 2HF may serve as a potential adjuvant treatment for BC patients.

RLIP, encoded by the Ral-binding protein-1 gene (*RALBP1*) is an ATPase that functions a transporter in the mercapturic acid pathway and an essential rate-regulating component of the clathrin-dependent endocytosis [30]. The main function of RLIP is to catalyze the transmembrane efflux of glutathione (GSH)-electrophile thioether conjugates (GS-Es) formed through the glutathione S-transferase-catalyzed conjugation of GSH with exogenous and endogenous electrophilic toxins [22,23,30,32]. As yet, no oncogene knockdown is reported to abrogate spontaneous carcinogenesis in rodent p53 homozygous knockout models. However, pharmacologically mediated partial suppression of RLIP protein prevents appearance of lymphoma or any other malignancy in p53 knockout homozygous mice [33]. In several solid cancers, RLIP protein levels are significantly higher than surrounding normal cells [17–19]. Further, RLIP plays an important role in regulating cytoskeletal dynamics in R-Ras-dependent cell spreading and migration [34]. RLIP-null fibroblasts migrate more slowly than wild-type cells in a scratch wound assay, and migration is restored in cells reconstituted with full-length RLIP [34]. These findings provide a rationale for studying the effectiveness of 2HF-mediated suppression of RLIP in inhibiting breast-to-lung metastasis in an orthotopic mouse model of BC.

In our study, 2HF inhibited the *in-vitro* growth of TNBC cells lines: MDA-MB231-luc, MDA-MB231Br-luc, and TMD231-luc. We further showed that 2HF impaired BC cell migration and invasion in wound healing and transwell cell invasion assays, respectively, and modulated the expression levels of several proteins, such as RLIP, pERK, KRAS, pP70S6K, and pSTAT3. The anti-metastatic potential of 2HF was further explored in an orthotopic mouse model of breast tumors. Indeed, the oral administration of 2HF suppressed the growth of primary breast tumors and inhibited metastasis to the lungs. Primary breast tumors from 2HF-treated mice exhibited reduced levels of RLIP protein expression, suggesting that 2HF may exert its anticancer effects by targeting RLIP. In addition, RLIP depletion or inhibition by RAS or Rab, respectively, led to greater reductions in primary tumor growth and metastasis to the lungs. Further, 2HF in combination with RAS and Rab led

to significantly smaller tumors than single-agent treatment, and completely blocked the incidence of metastasis to the lungs. Western blot analysis and immunohistochemistry further revealed that low levels of RLIP in response to 2HF treatment were associated with decreased phosphorylation (activation) of Akt and ERK, reduced protein expression levels of proliferation and cell-cycle associated proteins such as Ki67 and CDK4, inhibition of the angiogenesis marker CD31, low levels of the anti-apoptotic protein Bcl2, and high expression of the pro-apoptotic protein Bax. 2HF-treated cells also exhibited high expression of E-cadherin and low expression of vimentin, indicating the inhibition of EMT in tumor tissues.

In summary, this study demonstrated the anti-proliferative effects of 2HF in TNBC cells *in-vitro* and *in-vivo*. Our study presents a novel role for 2HF in inhibiting BC metastasis by suppressing RLIP, a stress-responsive oncogenic protein. Taken together, our results indicate that 2HF suppresses lung metastasis of BC cells, both alone and in combination with RLIP-targeting strategies. Further studies to identify the molecular mechanisms by which 2HF exerts its anti-metastatic effects are needed to establish its potential for use in clinical settings.

5. Significance

The results of our *in-vitro* and *in-vivo* studies suggest for the first time that 2HF has strong potential for the treatment of metastatic BC, and that it can potentiate the efficacy of RLIP depletion/inhibition via RLIP antisense and antibodies. Overall, this study shows that 2HF regulates the expression of numerous proteins in human BC cells, which may explain, in part, the therapeutic potential for 2HF. On the basis of our findings, further-in-depth studies are needed to decipher the mechanisms by which 2HF serves as an anticancer agent in BC. In addition, a better understanding of how 2HF might be used in combination with existing chemotherapies is required to consider its potential as an anticancer agent for clinical use.

Acknowledgements:

This work was supported in part by a Department of Defense grant (W81XWH-16-1-0641) and the Beckman Research Institute of City of Hope. The authors are grateful to Dr. Jun Wu (Tumor Biology Core Lab, City of Hope) for technical assistance with mammary fat pad injections and animal imaging. We sincerely thank Dr. Ravi Salgia, MD, PhD, Professor and Chair, Department of Medical Oncology at City of Hope, for providing research space and support.

Abbreviations:

BC	breast cancer
CAS	control antisense
EMT	epithelial-mesenchymal transition
ER	estrogen receptor
GSH	glutathione
GS-E	glutathione-electrophile conjugate

2HF	2’-hydroxyflavanone
Luc	luciferase
NSG	NOD scid gamma
PIS	pre-immune serum
PR	progesterone receptor
TNBC	triple-negative breast cancer
Rab	RLIP antibody
RAS	RLIP antisense
RLIP	a 76 kDa RAL-interacting protein
siRNA	small interfering RNA
STR	short tandem repeat

References

[1]. Senkus E, Cardoso F, Pagani O, Time for more optimism in metastatic breast cancer? Cancer Treat. Rev 40 (2014) 220–228. [PubMed: 24126121]

[2]. Liu X, Meng QH, Ye Y, Hildebrandt MAT, Gu J, Wu X, Prognostic significance of pretreatment serum levels of albumin, LDH and total bilirubin in patients with non-metastatic breast cancer, Carcinogenesis 36 (2015) 243–248. [PubMed: 25524924]

[3]. Yao H, He G, Yan S, Chen C, Song L, Rosol TJ, et al. , Triple-negative breast cancer: is there a treatment on the horizon? Oncotarget 8 (2017) 1913–1924. [PubMed: 27765921]

[4]. Zeichner SB, Terawaki H, Gogineni K, A review of systemic treatment in metastatic triple-negative breast cancer, Breast Cancer 10 (2016) 25–36. [PubMed: 27042088]

[5]. Song JK, Bae JM, Citrus Fruit Intake and Breast Cancer Risk: A quantitative systematic review, J. Breast Cancer 16 (2013) 72–76. [PubMed: 23593085]

[6]. Singhal J, Singhal P, Horne D, Salgia R, Awasthi S, Singhal SS, Metastasis of breast tumor cells to brain is suppressed by targeting RLIP alone and in combination with 2’-hydroxyflavanone, Cancer Lett. 438 (2018) 144–153. [PubMed: 30223070]

[7]. Nagaprashantha L, Adhikari R, Singhal J, Chikara S, Awasthi S, Horne D, et al. , Translational advances and opportunities for broad-spectrum natural phytochemicals and targeted agent combinations in breast cancer, Int. J. Cancer 142 (2018) 658–670. [PubMed: 28975625]

[8]. Singhal J, Nagaprashantha L, Chikara S, Awasthi S, Horne D, Singhal SS, 2’-Hydroxyflavanone: A novel strategy for targeting breast cancer, Oncotarget 8 (2017) 75025–75037. [PubMed: 29088842]

[9]. Nagaprashantha L, Singhal J, Li H, Warden C, Liu X, Horne D, et al. , 2’-Hydroxyflavanone effectively targets RLIP76-mediated drug transport and regulates critical signaling networks in breast cancer, Oncotarget 9 (2018) 18053–18068. [PubMed: 29719590]

[10]. Zhu J, Wu K, Chen Y, Ning Z, Zhang K, Du Y, et al. , Inhibitory effect of 2’-hydroxyflavanone on proliferation, invasion and migration of bladder cancer cells *in vitro via* blocking AKT/STAT3 signaling pathway,” Xi Bao Yu Fen Zi Mian Yi Xue Za Zhi 30 (2014) 237–240. [PubMed: 24606737]

[11]. Shin SY, Kim JH, Lee JH, Lim Y, Lee YH, 2’-Hydroxyflavanone induces apoptosis through Egr-1 involving expression of Bax, p21, and NAG-1 in colon cancer cells, Mol. Nutr. Food Res 56 (2012) 761–774. [PubMed: 22648623]

[12]. Nagaprashantha L, Vatsyayan R, Singhal J, Lelsani P, Awasthi YC, Prokai L, et al. , 2-Hydroxyflavanone inhibits proliferation, tumor vascularization and promotes normal differentiation in *VHL* mutant renal cell carcinoma, Carcinogenesis 32 (2011) 568–575. [PubMed: 21304051]

[13]. Singhal SS, Singhal J, Figarola JL, Riggs A, Horne D, Awasthi S, 2'-Hydroxyflavanone: A promising molecule for kidney cancer prevention, Biochem. Pharmacol 96 (2015) 151–158. [PubMed: 25957660]

[14]. Hsiao YC, Kuo WH, Chen PN, Chang HR, Lin TH, Yang WE, et al. , Flavanone and 2'-OH flavanone inhibit metastasis of lung cancer cells *via* down-regulation of proteinases activities and MAPK pathway, Chem. Biol. Interact 167 (2007) 193–206. [PubMed: 17376416]

[15]. Ofude M, Mizokami A, Kumaki M, Izumi K, Konaka H, Kadono Y, et al. , Repression of cell proliferation and androgen receptor activity in prostate cancer cells by 2'-hydroxyflavanone, Anticancer Res. 33 (2013) 4453–4461. [PubMed: 24123015]

[16]. Wu K, Ning Z, Zhou J, Wang B, Fan J, Zhu J, et al. , 2'-hydroxyflavanone inhibits prostate tumor growth through inactivation of AKT/STAT3 signaling and induction of cell apoptosis, Oncol. Rep 32 (2014) 131–138. [PubMed: 24859932]

[17]. Wang CZ, Yuan P, Xu B, Yuan L, Yang HZ. Liu X, RLIP76 expression as a prognostic marker of breast cancer, Eur. Rev. Me. Pharmacol. Sci 19 (2015) 2105–2111.

[18]. Wang Q, Wang JY, Zhang XP, Lv ZW, Fu D, Lu YC, et al. , RLIP76 is overexpressed in human glioblastomas and is required for proliferation, tumorigenesis and suppression of apoptosis, Carcinogenesis 34 (2013) 916–926. [PubMed: 23276796]

[19]. Singhal SS, Awasthi YC, Awasthi S, Regression of melanoma in a murine model by RLIP76 depletion, Cancer Res. 66 (2006) 2354–2360. [PubMed: 16489041]

[20]. Stuckler D, Singhal J, Singhal SS, Yadav S, Awasthi YC, Awasthi S, RLIP76 transports vinorelbine and mediates drug resistance in non-small cell lung cancer, Cancer Res. 65 (2005) 991–998. [PubMed: 15705900]

[21]. Singhal SS, Singhal J, Yadav S, Dwivedi S, Boor PJ, Awasthi YC, et al. , Regression of lung and colon cancer xenografts by depleting or inhibiting RLIP76 (Ral-binding protein 1), Cancer Res. 67 (2007) 4382–4389. [PubMed: 17483352]

[22]. Awasthi S, Singhal SS, Awasthi YC, Martin B, Woo JH, Cunningham CC, et al. , RLIP76 and Cancer, Clin. Cancer Res 14 (2008) 4372–4377. [PubMed: 18628450]

[23]. Awasthi S, Singhal SS, Pikula S, Piper JT, Srivastava SK, Torman RT, et al. , Novel function of human RLIP76: ATP-dependent transport of glutathione conjugates and doxorubicin, Biochemistry 39 (2000) 9327–9334. [PubMed: 10924126]

[24]. Singhal SS, Singhal J, Yadav S, Sahu M, Awasthi YC, Awasthi S, RLIP76: A target for kidney cancer therapy, Cancer Res. 69 (2009) 4244–4251. [PubMed: 19417134]

[25]. Singhal SS, Singhal J, Figarola JL, Horne D, Awasthi S, RLIP76 targeted therapy for kidney cancer, Pharm. Res 32 (2015) 3123–3136. [PubMed: 26021465]

[26]. Singhal SS, Roth C, Leake K, Singhal J, Yadav S, Awasthi S, Regression of prostate cancer xenografts by RLIP76 depletion, Biochem. Pharmacol 77 (2009) 1074–1083. [PubMed: 19073149]

[27]. Singhal SS, Jain D, Singhal P, Awasthi S, Singhal J, Horne D, Targeting the mercapturic acid pathway and vicenin-2 for prevention of prostate cancer, Biochim. Biophys. Acta 1868 (2017) 167–175.

[28]. Zhong W, Owens C, Chandra N, Popovic K, Conaway M, Theodorescu D, RalBP1 is necessary for metastasis of human cancer cell lines, Neoplasia 12 (2010) 1003–1012. [PubMed: 21170262]

[29]. Chikara S, Lindsey K, Dhillon H, Mamidi S, Kittilson J, Christofidou-Solomidou M, et al. , (2017) Enterolactone induces G_1-phase Cell cycle arrest in non-small cell lung cancer cells by down-regulating cyclins and cyclin-dependent kinases, Nutr. Cancer 69 (2017) 652–662. [PubMed: 28323486]

[30]. Singhal SS, Wickramarachchi D, Yadav S, Singhal J, Leake K, Vatsyayan R, et al. , Glutathione-conjugate transport by RLIP76 is required for clathrin-dependent endocytosis and chemical carcinogenesis, Mol. Cancer Ther 10 (2011) 16–28. [PubMed: 21220488]

[31]. Hsiao YC, Hsieh YS, Kuo WH, Chiou HL, Yang SF, Chiang WL, et al. , The tumor-growth inhibitory activity of flavanone and 2′-OH flavanone *in vitro* and *in vivo* through induction of cell cycle arrest and suppression of cyclins and CDKs, J. Biomed. Sci 14 (2007) 107–119. [PubMed: 17031514]

[32]. Singhal SS, Singh SP, Singhal P, Horne D, Singhal J, Awasthi S, Antioxidant role of glutathione s-transferases: 4-hydroxynonenal, a key molecule in stress-mediated signaling, Toxicol. Appl. Pharmacol 289 (2015) 361–370. [PubMed: 26476300]

[33]. Awasthi S, Tompkins J, Singhal J, Riggs AD, Yadav S, Wu X, et al. , RLIP depletion prevents spontaneous neoplasia in TP53 null mice, Proc. Natl. Acad. Sci 115 (2018) 3918–3923. [PubMed: 29572430]

[34]. Wurtzel JG, Lee S, Singhal SS, Awasthi S, Ginsberg MH LE Goldfinger, RLIP76 regulates Arf6-dependent cell spreading and migration by linking ARNO with activated R-Ras at recycling endosomes, Biochem. Biophys. Res. Commun 4 (2016) 785–791.

Highlights

- RLIP, a potential molecular target in breast cancer (BC)
- RLIP inhibition reduces *in-vitro* cell-viability and suppresses migratory and invasive potential of BC cells.
- RLIP inhibition/depletion suppresses primary breast tumor growth and its metastasis to lung.
- 2HF downregulate RLIP and Kras and their associated signal transduction pathways such as ERK, Stat3, and P70S6K

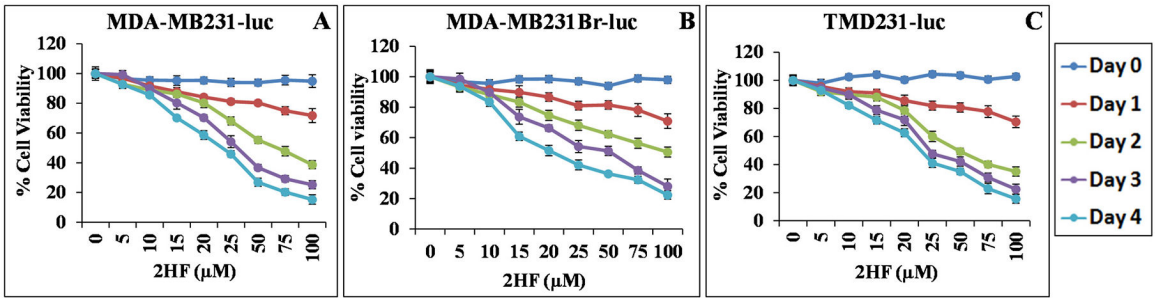

Figure 1. Effects of 2HF on the growth of BC cell lines.

The three BC cell lines **(A)** MDA-MB231-luc, **(B)** MDA-MB231Br-luc, and **(C)** TMD231-luc were treated with increasing concentrations of 2HF (0 −100 μM) for up to 4 days. The data shown represent the average percentage of cell viability relative to control ± standard deviation from eight replicate wells per treatment in three independent experiments. The relative standard deviation (where applicable) was less than 8% in all cases. Statistically significant differences were determined using Student's *t*-tests; $p<0.05$, 2HF-treated compared to untreated controls.

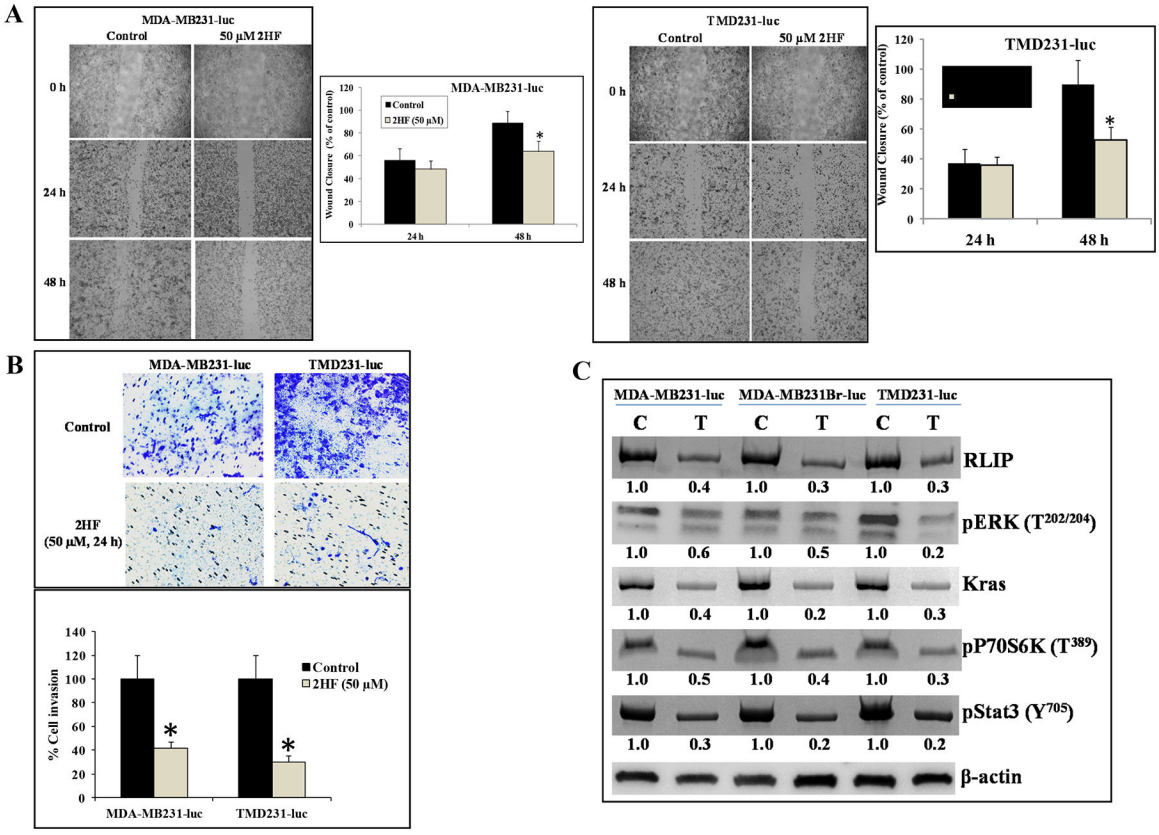

Figure 2. Effects of 2HF on the migration and invasion of BC cell lines.

(A) MDA-MB231-luc and TMD231-luc BC cells were grown to ~90% confluency in cell culture dishes. A scratch/wound was made in each dish. The cells were then treated with 2HF (50 μM). Images were taken at each time point for the respective control and treatment groups. The distance across the wound was measured in three replicate experiments and quantified as the percentage of wound closure. **(B)** MDA-MB231-luc and TMD231-luc BC cells were placed in the upper chamber of Matrigel inserts (8 μm pore size) in serum-free RPMI-1640 medium and treated with 2HF (50 μM) for 24 h. Invasive cells were fixed with 4% paraformaldehyde, stained with 0.2% crystal violet, and photographed under a light microscope at 200x. Invasive 2HF-treated cells were quantified and normalized to the percentage of invasive control DMSO-treated cells. **(C)** MDA-MB231-luc, MDA-MB231Br-luc, and TMD231-luc BC cells were treated with 2HF (50 μM) for 24 h. Western blot analysis was performed to identify changes in protein levels of RLIP, pERK ($T^{202/204}$), KRAS, pP70S6K (T^{389}), and pSTAT3 (Y^{705}). Numbers below the blots indicate the fold differences in the levels of proteins as compared to control as determined by densitometry. β-actin was used as a loading control.

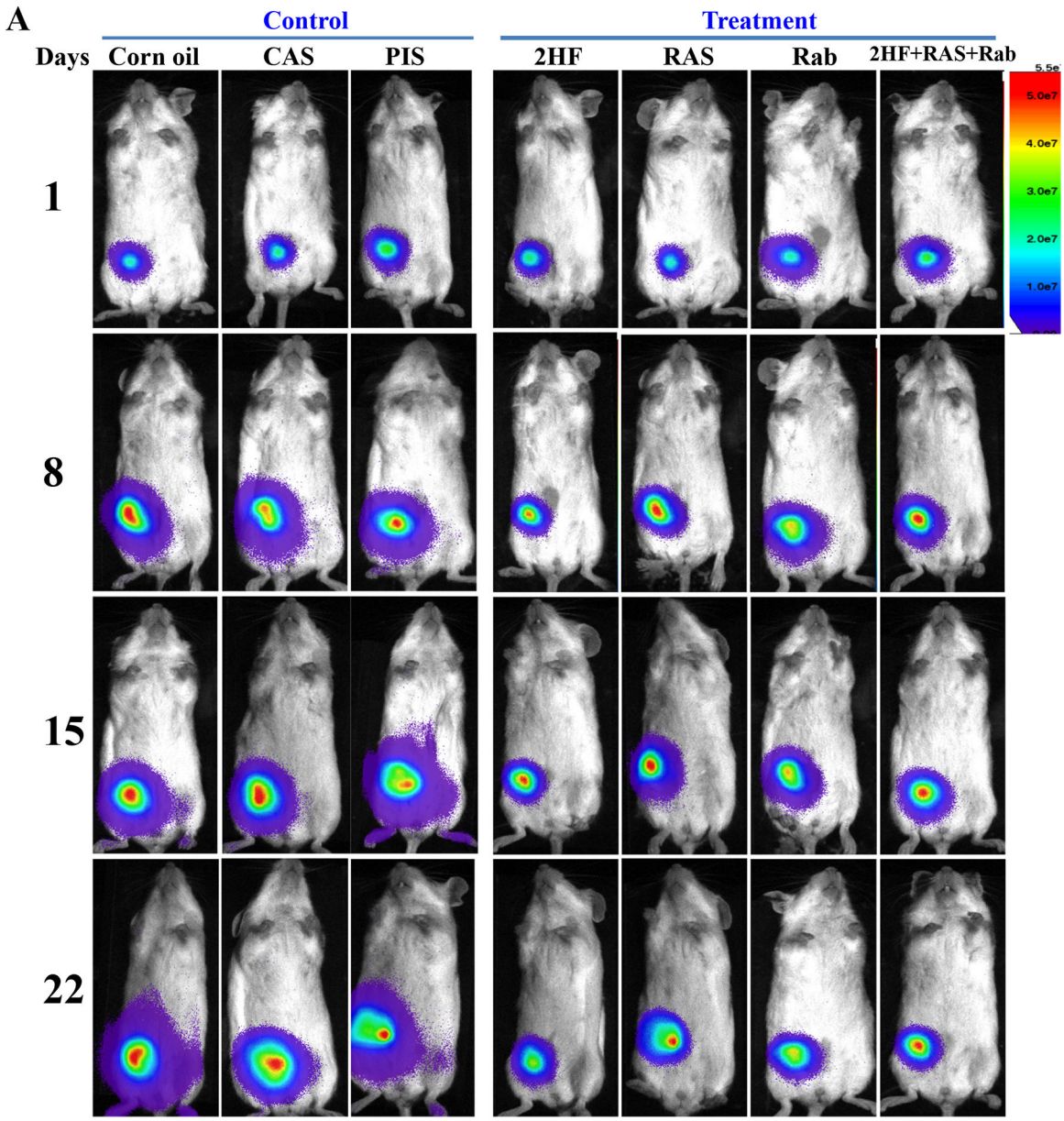

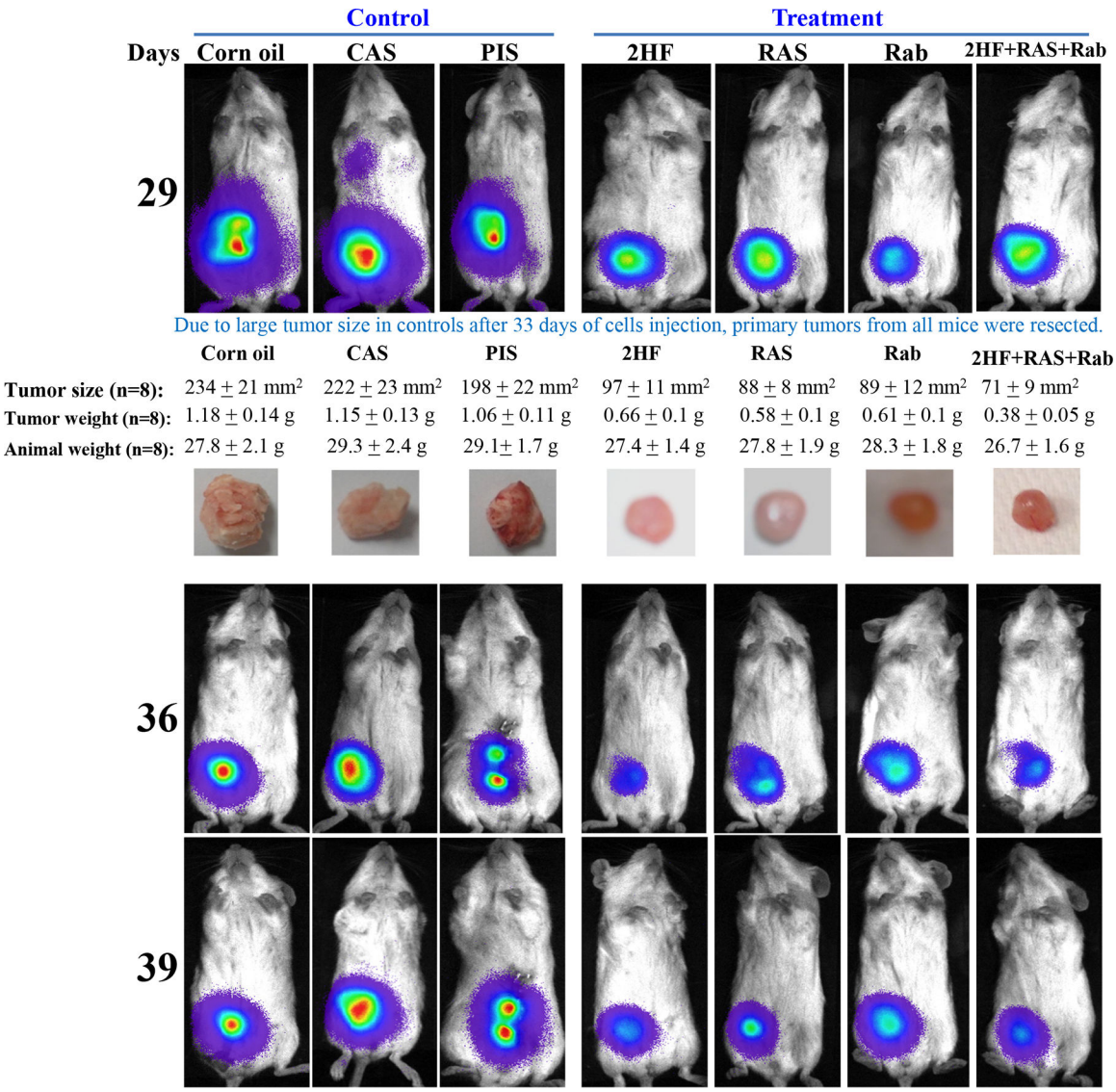

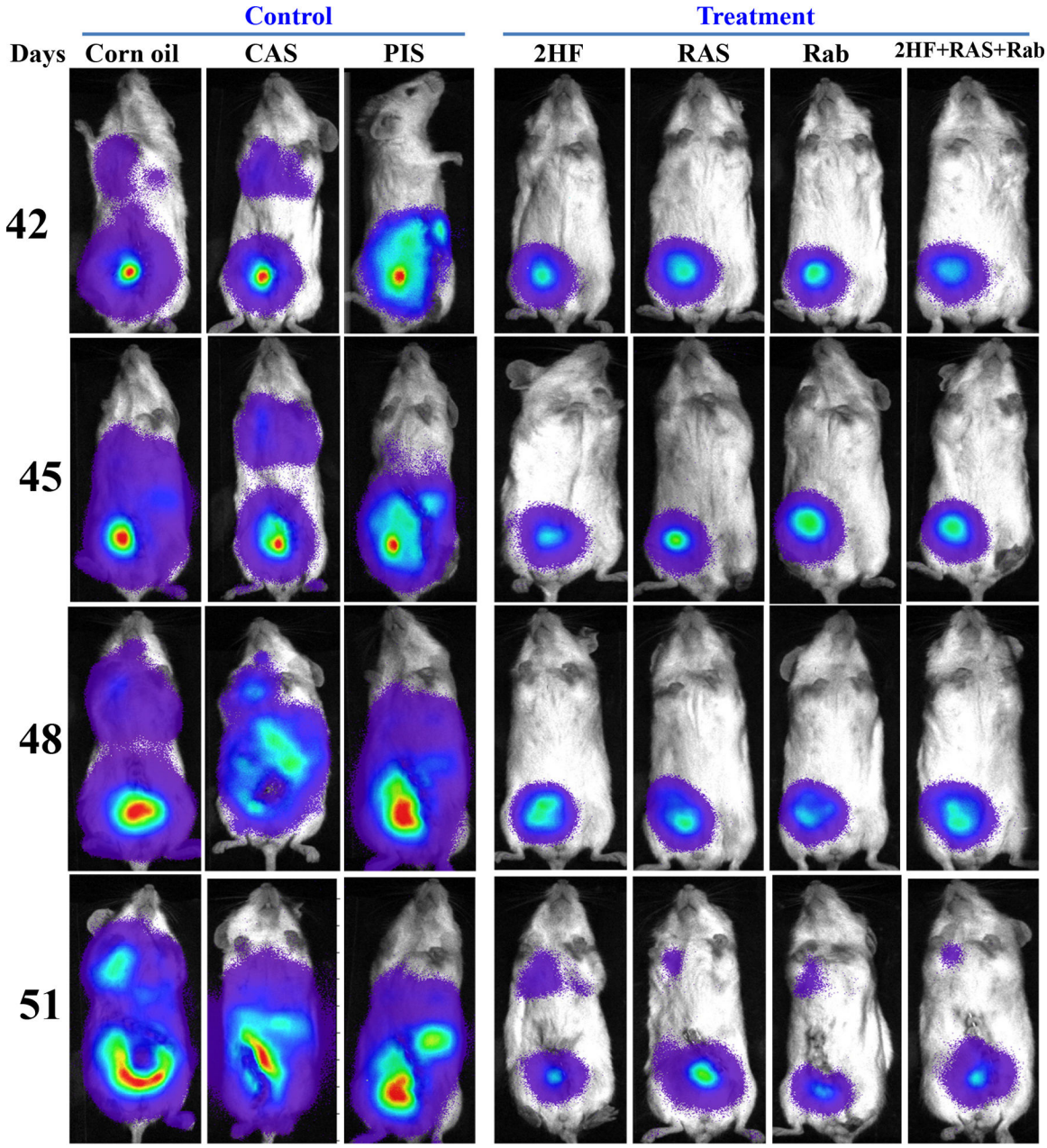

Due to large tumor size and metastasis occur in all controls at day 51 of cells injection, all animals were euthanized; collect tumor and tissues, measure tumor size and weight were recorded.

	Corn oil	CAS	PIS	2HF	RAS	Rab	2HF+RAS+Rab
Tumor size (n=8):	284 ± 28 mm²	269 ± 32 mm²	259 ± 27 mm²	91 ± 12 mm²	80 ± 9 mm²	84 ± 10 mm²	62 ± 7 mm²
Tumor weight (n=8):	1.85 ± 0.19 g	1.73 ± 0.18 g	1.47 ± 0.15 g	0.61 ± 0.1 g	0.52 ± 0.1 g	0.53 ± 0.1 g	0.29 ± 0.04 g
Animal weight (n=8):	32.7 ± 2.4 g	34.2 ± 2.8 g	33.7 ± 1.9 g	31.8 ± 2.1 g	30.2 ± 1.8 g	31.5 ± 1.6 g	29.3 ± 1.5 g

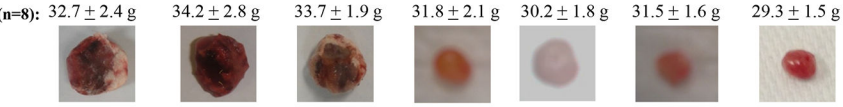

B

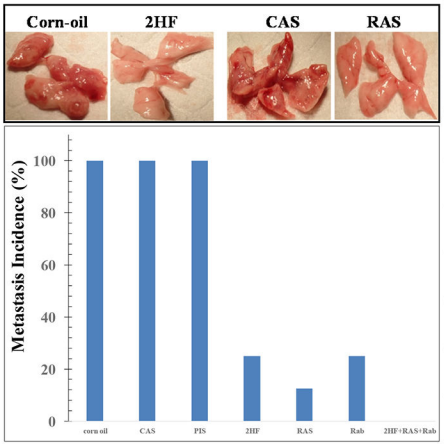

C

Groups	Average No. (Range) of Lung Metastases	Average No. (Range) of Liver Metastases
Corn oil	15.5 (8-23)	33.3 (19-46)
CAS	14.7 (8-23)	38.2 (27-52)
PIS	15.6 (11-22)	41.3 (29-56)
2HF	0.3 (0-3)	1.8 (0-8)
RAS	0	0.7 (0-6)
Rab	0.2 (0-2)	1 (5-8)
2HF+RAS+Rab	0	0

Figure 3. Effects of 2HF, RAS, Rab, and their combination treatment on primary tumor growth and lung metastasis.

(A) TMD231-luc (lung-seeking) BC cells were injected into the fourth mammary fat pad of NSG mice randomized into 7 treatment groups (corn oil, CAS, PIS, 2HF, RAS, Rab, and 2HF+RAS+Rab; n=8/ group). Mice in the control groups received either corn oil via oral gavage on alternate days or CAS or PIS via *i.p.* weekly; mice in the treatment groups received either 2HF (50 mg/kg b.w.) in corn oil by oral gavage on alternate days or RAS (5 mg/kg b.w.) or Rab (5 mg/kg b.w.) via *i.p.* weekly. *In-vivo* bioluminescent imaging was used to monitor metastasis in the mice twice a week after the BC cell injection. The bioluminescence intensity scale is shown on the right. Tumor size (cross-sectional area), tumor weight, and animal weight for each group are shown for Day 33 (when primary tumors were resected to reduce tumor burden and allow time for metastasis) and Day 51. **(B)** Images of representative mouse lungs (from the mice presented in panel A) dissected after necropsy. The numbers of surface lung tumor nodules, indicative of BC metastasis, were counted and reported as percent incidence. **(C)** Tumors in the liver were also counted after necropsy at Day 51.

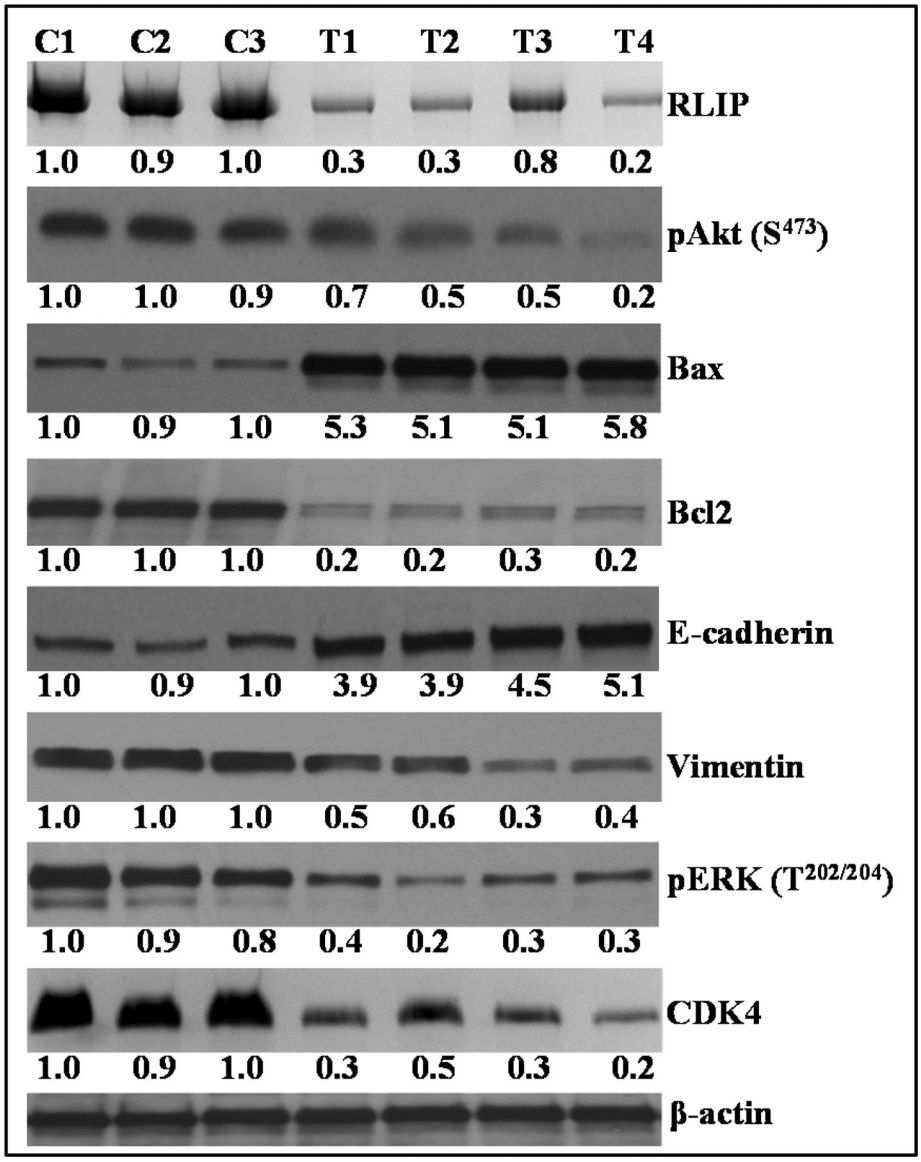

Figure 4. Effects of 2HF on protein expression in tumor tissues.

Primary tumor tissue excised from mice in the control groups - corn oil (**C1**), CAS (**C2**), PIS (**C3**); treatment groups - 2HF (**T1**), RAS (**T2**), Rab (**T3**), and 2HF+RAS+Rab (**T4**) was analyzed for differences in the expression levels of RLIP, pAkt, Bax, Bcl2, E-cadherin, vimentin, pERK, and CDK4. β-actin was used as a loading control. Numbers below the blots indicate the fold differences in protein expression in the treated tissues compared to in control tissues as determined by densitometry.

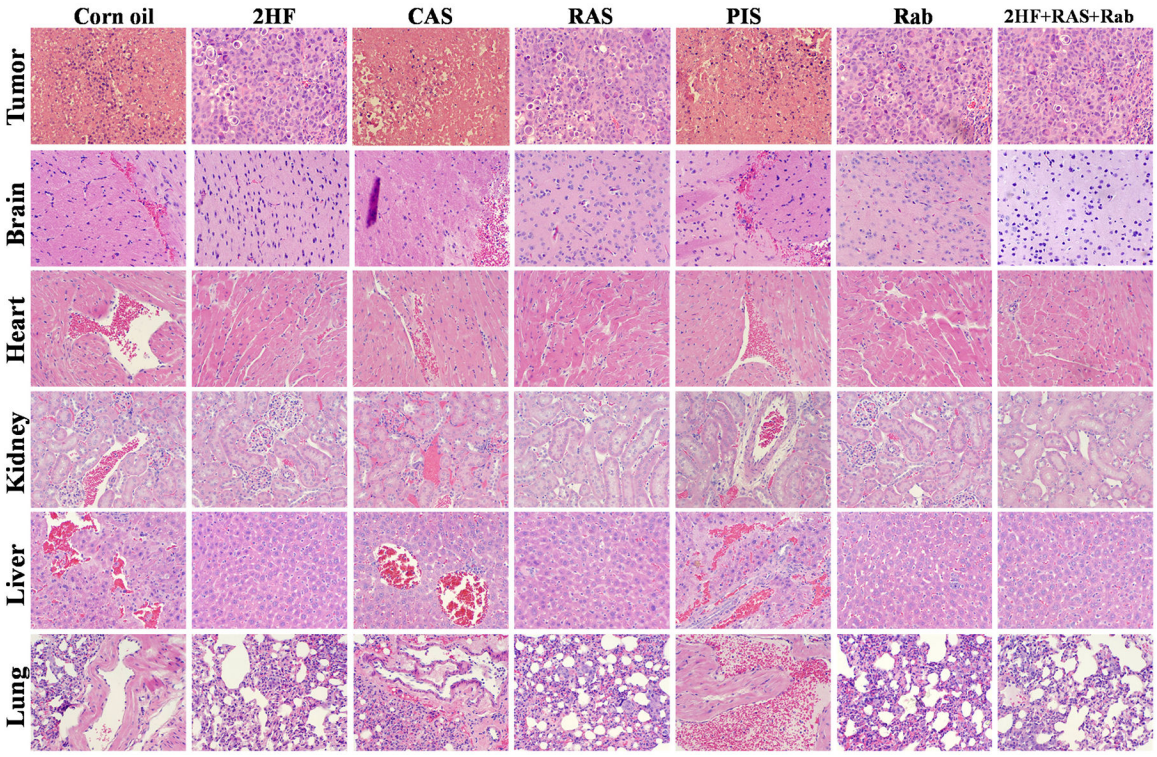

Figure 5. Effects on the morphology of tumors and other organs excised at day 51 from TMD231-luc BC orthotopic mammary fatpad injected NSG mice:

Control treated (corn oil, CAS, and PIS) and experimental treated (2HF, RAS, Rab, and 2HF+RAS+Rab) groups bearing NSG mice tumors and other tissues sections were used for H & E staining. Hemorrhagic areas involving the liver, lung, kidney and heart tissues were observed in the control-treated mice whereas tissues from experimental-treated mice were histologically normal. **2HF**, 2'-hydroxyflavanone treated; **CAS,** control antisense treated; **RAS,** RLIP antisense treated; **PIS,** pre immune serum treated; **Rab,** RLIP antibody treated.

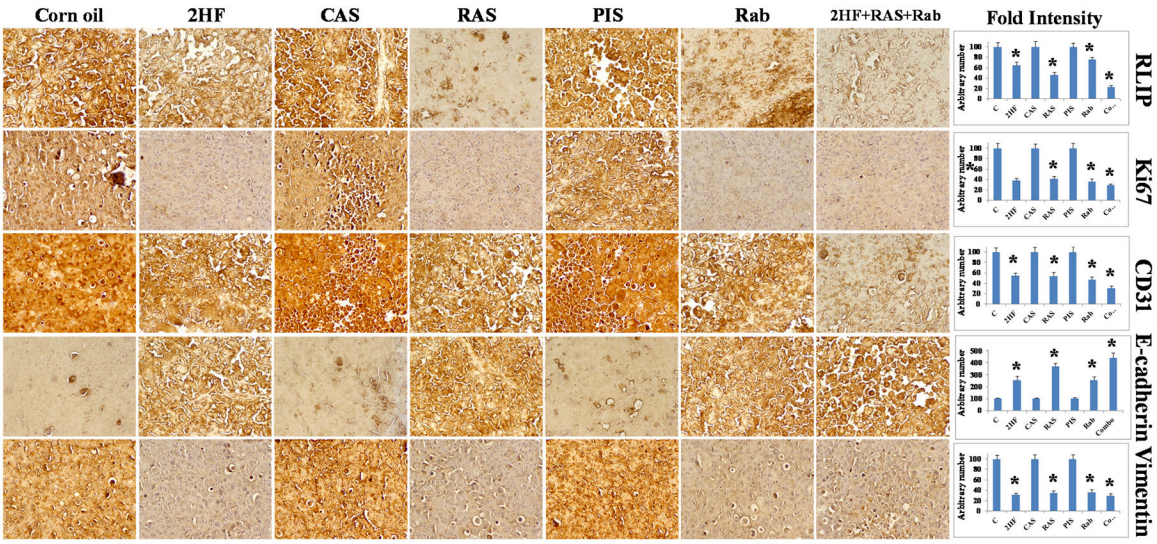

Figure 6. Immunohistochemistry of tumor tissue from mice in the control and experimental treatment groups.

Immunohistochemistry was performed to detect RLIP, Ki67, CD31, E-cadherin, and vimentin on primary tumor tissue isolated from mice in the control (corn oil, CAS, PIS) and experimental (2HF, RAS, Rab, and 2HF+RAS+Rab) treatment groups. The intensity of antigen staining was quantified by digital image analysis using Pro Plus software. Bars represent mean ± S.E. (n = 5). One representative image for each treatment group is shown. *Statistically significant differences were determined using two-tailed Student's *t* tests; $p < 0.01$, 2HF-, Rab-, and RAS-treated compared to their respective controls.